2007 IEEE International Conference on
Robotics and Automation
Roma, Italy, 10-14 April 2007

Kinematic Design and Dynamic Analysis of a Planar Biped Robot Mechanically Coordinated by a Single Degree of Freedom

J. McKendry, B. Brown, E.R. Westervelt, and J.P. Schmiedeler

Abstract— **This paper presents a method of integrating kinematic mechanism design and hybrid system analysis for the design of a single-degree-of-freedom (DOF) planar biped robot that can achieve dynamic walking gaits that are stable. Reducing the DOF in a biped can result in a reduction of the complexity of the control strategies needed to enable stable walking. Although the biped designed by this procedure is restricted to a single gait, this biped may be less complex, lighter, and less costly to construct than one whose multiple DOF are coordinated via feedback.**

I. Introduction

A. Background

Over the past thirty years, a large assortment of biped robots have been constructed with varying levels of design complexity. As an example of the highly complex, consider Honda's Asimo, a humanoid that can achieve a variety of gaits in three dimensions using the twelve actuated degrees of freedom (DOF) in its legs. At the other extreme is a class of bipedal robots called passive-dynamic walkers. These robots are able to walk stably down a slope and require gravity as their only source of energy [5]. Between these two extremes exist many robots that employ reduced actuation strategies and whose motions are restricted to the sagittal plane. For example, consider RABBIT [1], a planar biped that requires only four actuators to effect walking in its five DOF. Collins et al. [2] take reduced actuation further in their set of walkers that are actuated solely at the ankles and closely approximate passive-dynamic gaits. As another example, Ono et. al. [6] apply principles of self-excitation to create a planar biped that requires a single actuator. While all of the above machines can walk with human-like gaits, they accomplish this task in a variety of ways, including their actuation strategies. To date, a biped robot with point feet has yet to be constructed that can achieve human-like, dynamic[1] gaits by mechanically coordinating its motion with a single DOF.

B. Mechanism-Coordinated Motion

Mechanical coordination of motion has been explored in the past. Consider Rygg's mechanical horse [7] or Wan and Song's cam-controlled leg [9]. In the work presented in this paper, the idea of mechanical coordination used by Rygg and Wan and Song is taken to an extreme. Compared with Collins' work [2], which also examines minimizing the required actuation, the methods presented in this paper allow for active coordination of all leg degrees of freedom using a single input. The obvious disadvantage of reducing the DOF in this manner is the restriction of the biped's motion to a single gait. Despite this restriction, such a design has a number of benefits. First, the robust design is not limited to a single speed but is capable of a range of speeds near the design speed. Second, the motion control of the robot is simplified significantly. Additionally, a reduction in the number of actuators needed decreases the robot's weight and the number of sensors required.

Using tools from standard kinematic synthesis [4], it is possible to design a single-DOF mechanism that approximates the motions of a single leg over the duration of a biped's gait. By composing two identical mechanisms and applying appropriate constraints, one may design a planar biped robot in which the walking motions are coordinated by a single DOF. Dynamic properties can be assessed using known techniques [11], and the design may be refined such that the biped may walk with a gait that is dynamically stable. Figure 1 gives a 3D rendering of a single-DOF biped that has been designed using the methods presented in this paper.

Fig. 1. 3D rendering of a single-DOF biped. The biped's design results in the need for only a single actuator. Since the biped is planar, frontal plane stability is ensured by including a third leg whose motion is slaved to the motion of the other outer leg. Note that the inertial properties of the outer two legs combined must match those of the inner leg.

All authors are with the ME Department at The Ohio State University, Columbus, Ohio 43210, USA, {McKendry.8, Brown.2225, Westervelt.4, Schmiedeler.2}@osu.edu.

[1]Here, "dynamic gait" refers to a gait in which the biped's foot-rotation indicator point [3] is outside of the support polygon.

C. A Dynamic Model of Walking

A walking gait consists of successive strides, with each stride consisting of two steps. Each step may then be further broken down into two distinct phases: single support and double support. *Single support* is defined as the portion of the step in which only one leg (mechanism) is in contact with the ground. During this phase, the leg that is in contact with the ground is referred to as the *stance leg* while the other leg is called the *swing leg*. *Double support* is the portion of the step in which both legs (mechanisms) are in contact with the ground.

Here, double support is assumed to be instantaneous and is modeled as a rigid impact. Thus, the dynamic model of walking consists of successive phases of single support separated by impulsive transitions associated with foot touchdown and is therefore hybrid.

D. Paper Organization

Section II of this paper presents the methods of kinematic synthesis. The section describes how to design a single-DOF mechanism that approximates a target set of walking motions for a single leg. The section then details the design of a single-DOF biped robot through the composition of two identical mechanisms. Section III presents the methods of dynamic analysis. The equations of motion governing single support and the transition mapping to be applied between steps are derived. Optimization of the robot's kinematic, dynamic, and control parameters to meet desired dynamic and mechanical constraints is also discussed. In Section IV, an example design is given. Simulation results are then presented and discussed. Concluding remarks are presented in Section V.

II. Kinematic Synthesis

A. Selecting a Desired Walking Motion

The first step in the design process is to select a gait to be used as a target for the single-DOF mechanism design. The gait may be obtained from a variety of sources, for example, a known stable gait from a biped or human gait data. The gait is used as a target motion for the initial mechanism design. Since this initial design only considers the biped's kinematics, optimization may be used to refine the design after the biped's dynamics are considered to produce a dynamic gait that is stable.

B. Mechanism Design and Composition

1) Single Leg Mechanism Design: The mechanism is initially designed to approximate the target motion. The number of links and their configuration may be decided upon with the aid of a linkage analysis software package. When designing, appropriate links should be selected to represent the body and the leg segments. For example, to approximate the motion of the femur throughout a walking gait, a four-bar linkage may be selected such that the crank is the input, the mechanism's base link is the body, and the rocker is the femur. If the motion of the tibia is also of interest, the design process can be simplified by first designing the femur mechanism and then building off of that mechanism to incorporate the tibia motion as well; this is the approach taken in the example (see Section IV).

The mechanism designed is assumed to satisfy the following constraints:

- CK1) The mechanism is planar and composed of N rigid links connected by revolute or prismatic joints.
- CK2) The mechanism contacts the ground at only one point.
- CK3) A reference frame is selected such that all link angles may be measured with respect to that frame.
- CK4) Relative to any link, the mechanism is 1 DOF.
- CK5) The link angles of all links can be found as analytical functions of the known quantities: the angle of the input link, the absolute orientation of one link, all of the link lengths, and any constant internal link angles.

Once the mechanism's configuration has been determined, the motions that the mechanism generates may be designed by varying the kinematic parameters (by optimization). Note that only the relationship between the link lengths—not the actual values—is significant since the motion generated is independent of the mechanism's scale.

2) Composing Two Single Leg Mechanisms: The processes given in Sections II-A and II-B.1 produce a mechanism that is parameterized by known quantities and approximates a given walking motion. Assuming the gait is symmetric, a biped robot can be designed by composing two separate mechanisms (each mechanism represents one leg of the robot). The mechanisms and their composition are assumed to satisfy the following constraints:

- CC1) The two mechanisms are identical.
- CC2) After composition, the two mechanisms share a common link.
- CC3) The two mechanisms are driven π radians out of phase.
- CC4) The stance leg mechanism is parameterized by the angle of its input link q_i and a link angle q_m that describes the mechanism's absolute orientation.
- CC5) The swing leg mechanism is parameterized by the angle of its input link $q_i + \pi$ and the angle of the link that the two mechanisms share q_b.

Since q_b is shared by both mechanisms, q_b of the swing leg may be written as an analytical function of q_i and q_m of the stance leg. Hence, the entire biped can be parameterized by q_i and q_m of the stance leg.

III. Dynamic Analysis & Optimization

A. Applying Dynamic Considerations to the Biped Model

To achieve dynamic walking that is stable, the dynamics of the biped must be considered. The design process presented in Section II is based purely on kinematics. It does not include dynamic considerations such as inertial and Coriolis effects, gravitational forces, and the impulsive contact forces associated with ground contact at double support. By considering the dynamics associated with the single support phase as well as the impacts, stability of the biped's gait design may be assessed.

B. Single Support Equations of Motion

Since the biped's forward kinematics are known, the equations of motion governing the single support phase may be readily derived using the method of Lagrange. The equations of motion are

$$D(q)\ddot{q} + C(q,\dot{q})\dot{q} + G(q) = \tau, \tag{1}$$

where $q := (q_i; q_m) \subset \mathbb{T}^2$, $D(q)$ is the mass-inertia matrix, $C(q,\dot{q})$ is the Coriolis matrix, $G(q)$ is the gravity vector, and τ is the vector of generalized forces. The model in state-space form is

$$\dot{x} = \begin{bmatrix} \dot{q} \\ D^{-1}(q)[-C(q,\dot{q})\dot{q} - G(q) + \tau] \end{bmatrix}, \tag{2}$$

where $x := (q; \dot{q})$.

C. Impact Mapping and Coordinate Relabeling

The swing leg end touchdown at double support is modeled as a rigid contact between two bodies. The transition model includes a relabeling of the coordinates so that the same model for single support (1) may be used irrespective of which leg is in contact with the ground. The impact model requires the generalized coordinates to be extended to include the Cartesian position of the contact point between the biped's stance leg and the ground. The extended model's generalized coordinates are taken to be $q_e := (q; x; y)$.

By modeling the contact between the swing leg and the ground as a rigid impact, it is assumed that the impulsive forces acting at the contact point will result in a change of the conjugate momenta of the generalized coordinates. Since the swing leg assumes the role of the stance leg at impact, the velocity of the swing leg end must be zero immediately after impact. These two assumptions may be expressed compactly as

$$\Pi^{-1}(q_e^-) \begin{bmatrix} \dot{q}_e^+ \\ \hat{f} \end{bmatrix} = \begin{bmatrix} D_e(q_e^-)\dot{q}_e^- \\ 0 \end{bmatrix}, \tag{3}$$

where

$$\Pi^{-1}(q_e^-) = \begin{bmatrix} D_e(q_e^-) & -J^T(q_e^-) \\ J(q_e^-) & 0 \end{bmatrix},$$

$\dot{q}_e^-$ and $\dot{q}_e^+$ are the velocities immediately before and after impact[2], respectively, $D_e(q_e^-)$ is the mass-inertia matrix of the extended model, $J(q_e^-)$ is the Jacobian of the swing leg end position in the extended model, and $\hat{f} = (\hat{f}_h; \hat{f}_v)$ denotes the vector consisting of the horizontal and vertical impulses acting at the contact point between the swing leg end and the ground. It may be shown that $\Pi^{-1}(q_e^-)$ is invertible. Since the mechanism under consideration is planar, calculation of the coordinate relabeling function due to the swapping of roles between the stance and swing legs at impact is trivial.

[2] The superscripts "$-$" and "$+$" are used from this point forward to denote values immediately before and after impact, respectively.

D. Additional Model Considerations

In addition to Constraints CK1–CK5 and CC1–CC5, the following constraints are imposed on the biped's gait:

- CG1) The angle q_m is strictly monotonic over the duration of a step.
- CG2) The normal ground reaction force is always directed upward.
- CG3) The ratio of the tangential component to the normal component of the ground reaction force does not exceed the coefficient of static friction at the contact point between the stance leg end and the walking surface.

Constraint CG1 will be key to the developments in Section III-E, while Constraint CG2 and CG3 ensure the stance leg of the robot will not lift off the ground or slip during single support.

E. Control

Using a feedback controller, the input angle q_i will be slaved to be a function of $\theta := q_m$. Since θ is strictly monotonic over the duration of a step per CG1, a variable s that parameterizes step progression may be defined as

$$s := \frac{\theta - \theta^+}{\theta^- - \theta^+}, \tag{4}$$

where θ^+ and θ^- correspond to the values of θ at the beginning and end of the step, respectively. Hence, s is monotonically increasing from $s = 0$ at step start to $s = 1$ at step end. The evolution of q_i with respect to s may be chosen to be some desired polynomial. Since s is a function of only θ, the desired polynomial may also be expressed as a function of only θ and is represented by $h_d(\theta)$. The result is a single-input, single-output system in which a computed torque or high-gain PD controller can be used to impose the slaving of q_i to θ.

F. Optimization of Walking Motions

To realize a stable gait, the biped's kinematic, dynamic, and control parameters must be appropriately chosen. Although it may be possible to choose the parameters by hand, constrained nonlinear parameter optimization may be used to make the parameter selection process systematic.

A variety of objective functions may be selected for optimization. An obvious choice is one that penalizes the required actuator torque. Considerations necessary to achieve stable and desirable walking motions are expressed as equality and inequality constraints. The equality constraints include constraints on

- EQ1) walking rate and
- EQ2) gait periodicity.

The inequality constraints include constraints on

IN1) ground contact forces (such that CG2 and CG3 are satisfied),

IN2) desirable actuator power requirements, and

IN3) link lengths, masses, and inertias (such that they are physically realizable, for instance, the link lengths must be positive).

G. Walking Gait Stability Analysis

The stability of the periodic motion found in Section III-F may be readily determined using the results of [10], [11], which makes use of two analysis tools: zero dynamics and Poincaré return maps. Next, a sketch of the results of [10], [11] specific to the biped's model will be given.

Consider the following coordinate transformation on the robot's state x,

$$\eta := \begin{bmatrix} y \\ \dot{y} \\ z_1 \\ z_2 \end{bmatrix} = \begin{bmatrix} q_i - h_d(\theta) \\ \dot{q}_i - \frac{\partial h_d}{\partial \theta}\dot{\theta} \\ \theta \\ \sigma_2 \end{bmatrix}, \tag{5}$$

where σ_2 is the angular momentum about the stance leg end. When the constraints are exactly imposed ($y \equiv 0$), the free dynamics that result (the zero dynamics) in the η coordinates are

$$\dot{z} = \begin{bmatrix} \dot{z}_1 \\ \dot{z}_2 \end{bmatrix} = \begin{bmatrix} \dot{\theta} \\ \dot{\sigma}_2 \end{bmatrix} = \begin{bmatrix} \kappa(z_1) z_2 \\ M_{\rm tot}\, g_o\, x_{\rm com}(z_1) \end{bmatrix}, \tag{6}$$

where $M_{\rm tot}$ is the total mass of the robot and $x_{\rm com}$ is the horizontal distance between the robot's center of mass and the stance leg end. The function κ may be shown to be only a function of z_1 (by inverting the coordinate transformation and setting $y \equiv 0$). Manipulation of (6) followed by integration results in

$$\frac{1}{2}(z_2^-)^2 = \frac{1}{2}(z_2^+)^2 - V_{\rm zero}(z_1^-), \tag{7}$$

where

$$V_{\rm zero}(z_1^-) := -\int_{z_1^+}^{z_1^-} \frac{M_{\rm tot}\, g_o\, x_{\rm com}(z_1)}{\kappa(z_1)}\, dz_1. \tag{8}$$

Using the impact model developed in Section III-C, the effect of the impact on z_2 may be written as

$$z_2^+ = \delta_{\rm zero} z_2^-, \tag{9}$$

where $\delta_{\rm zero}$ is a constant that accounts for the loss of momentum at impact. Using (7) and (9) and defining $\zeta_i := \frac{1}{2}z_i^2$, $i = 1, 2$, an expression relating ζ_2 at steps k and $k+1$ may be written as

$$\zeta_{2,k+1}^- = \delta_{\rm zero}^2 \zeta_{2,k}^- - V_{\rm zero}(z_1^-). \tag{10}$$

As long as

$$\zeta_2^- > \max_{z_1^+ \le z_1 \le z_1^-} \frac{V_{\rm zero}(z_1)}{\delta_{\rm zero}^2}, \tag{11}$$

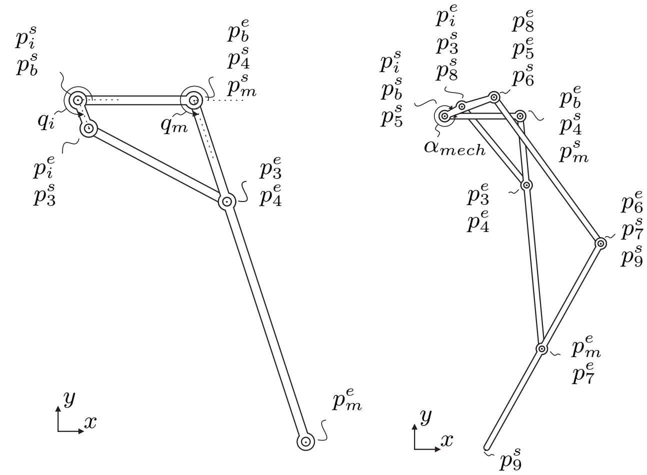

(a) Femur mechanism. (b) Leg mechanism.

Fig. 2. Mechanism schematics. The four-bar mechanism depicted in (a) was designed to approximate (only) the femur motion. The six-link mechanism depicted in (b) was designed to approximate the femur and tibia motions. The initial four-bar (femur) mechanism was unchanged (except for the input angle) when it was incorporated into the six-link mechanism. $\vec{r}_\star$ is a vector that extends from the starting point $p_\star^s$ to the ending point $p_\star^e$ of each link.

the discrete-time linear system (10), termed the restricted Poincaré return map, admits a fixed point ζ_2^{*-} given by

$$\zeta_2^{*-} = -\frac{V_{\rm zero}(z_1^-)}{1 - \delta_{\rm zero}^2}. \tag{12}$$

If the fixed point satisfies (11), it will be stable as long as

$$\delta_{\rm zero}^2 < 1. \tag{13}$$

IV. Example

A. Kinematic Design of an Example Biped

Experimental data from a 5-link biped designed by the authors [8] was selected for the target motion profiles. The trajectories that were chosen to be approximated were those of the femur and tibia (with respect to a fixed frame). To simplify the design process, a submechanism is first designed to approximate only the femur motion. This mechanism is a simple four-bar linkage, depicted in Figure 2(a). All angles are measured with respect to the positive x-axis and are denoted by $\vartheta_\star$. The link fixed to the body $\vec{r}_b$ is selected to be the base link so that $q_b := \vartheta_b$ describes the absolute orientation of the mechanism. Note also that the angle of the input link is defined as $q_i := \vartheta_i$ and the angle of the femur link is defined as $q_m := \vartheta_m$. While other mechanism designs were explored, for example, six-bar mechanisms, it was decided that the modest improvement in approximation of the desired femur motion did not warrant the complexities that would be added to both the kinematic and dynamic analyses.

Once the mechanism configuration was determined, each link was given a vector representation. After writing the vector loop equation,

$$\vec{r}_b + \vec{r}_4 = \vec{r}_i + \vec{r}_3, \tag{14}$$

the full position kinematics of the mechanism are known in terms of the link lengths, q_i, and q_b. This motion was then optimized to approximate the desired femur motion $\vartheta_m^d(s)$, $0 \leq s \leq 1$, over one step by using the objective function

$$f_{fem} = \int_0^1 (\vartheta_m(s) - \vartheta_m^d(s))^2 ds. \quad (15)$$

Link lengths $|\vec{r}_i|$, $|\vec{r}_3|$, and $|\vec{r}_4|$ were treated as variable parameters while the base link length $|\vec{r}_b|$ was held constant. Upper and lower bounds were placed on the design variables to maintain physically realizeable parameters. Note that $|\vec{r}_m|$ was not included since $\vartheta_4 = \vartheta_m$.

Once the femur mechanism was designed, the tibia mechanism was chosen to be a four-bar linkage as well. The tibia mechanism shares the same ground link as the femur mechanism and has the end of the femur link connected to the tibia creating a "knee". Additionally, the input links of the mechanism were combined to form a single rigid link. The resulting six-link mechanism is depicted in Figure 2(b). From the figure, the vector loop equation governing the kinematics of the tibia mechanism was identified as

$$\vec{r}_6 = \vec{r}_b + \vec{r}_m - \vec{r}_5 - \vec{r}_7. \quad (16)$$

It may be readily shown that the position kinematics for the entire mechanism may be determined in terms of the link lengths, the constant internal angle of the rigid driving link α_{mech}, q_b, and q_i.

To optimize the tibia motions, a new objective function for optimization, f_{tib}, was defined as

$$f_{tib} = \int_0^1 (\vartheta_9(s) - \vartheta_9^d(s))^2 ds, \quad (17)$$

where ϑ_9^d, $0 \leq s \leq 1$, is the desired tibia motion. All parameters determined in the femur motion optimization were treated as constant parameters while $|\vec{r}_m|$, $|\vec{r}_5|$, $|\vec{r}_6|$, $|\vec{r}_7|$, and α_{mech} were selected as the variable parameters. Again, upper and lower bounds were placed on the design variables. Note that $|\vec{r}_9|$ was not included since $\vartheta_7 = \vartheta_9$. For simplicity, the initial value for the tibia link length was selected such that $|\vec{r}_9| = |\vec{r}_m|$. Figure 3 gives a comparison of the mechanism-generated and target motion profiles.

Per CG1, the parameterizing angle describing the absolute orientation of the biped is required to be monotonically increasing over the duration of a step[3]. Since q_b was found to not meet this requirement, q_m, which did meet this requirement, was selected. The mechanism's kinematics were derived again by choosing the femur as the base link. By solving for the new unknowns, a mechanism parameterized by q_i and q_m was obtained. Two identical mechanisms (with different parameterizations) were then composed as specified in Section II-B.2. This resulting biped is depicted in Figure 1 (with an additional mechanism included to ensure symmetry about the frontal plane). The forward kinematics of this robot are expressed as functions of q_i and q_m of the stance leg.

[3]In terms of the mechanism input angle q_i, the duration of each step is π radians of rotation.

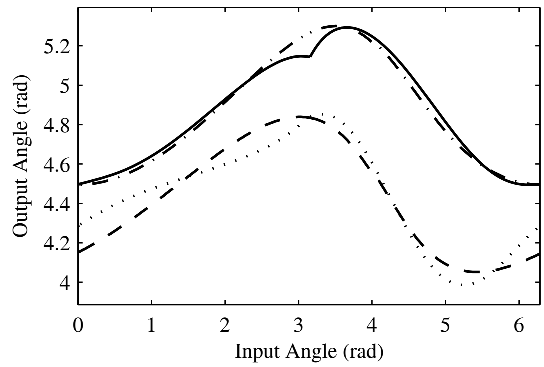

Fig. 3. Comparison of mechanism-generated (femur: dash-dot, tibia: dash) and target motions (femur: solid, tibia: dotted).

B. Dynamic Analysis and Simulation

Using the methods described in Section III, the dynamics of the model were analyzed using a MATLAB-based hybrid system simulator developed by the authors. The initial mass distribution was chosen such that the femur and tibia links were the most massive. The moments of inertia were calculated by approximating each link as a uniform slender rod. Even though the motion that resulted from this initial design differed from the target gait once dynamic effects were accounted for, the design nearly satisfied the conditions for stability, (11) and (13). The design was then optimized to minimize the cost function

$$f_{cost} = \int_0^T u^4(t) dt, \quad (18)$$

where $u(t)$ is the required torque of the (single) actuator and T is total time to complete the step. Here $u(t)$ is raised to the fourth power to approximately penalize peak control effort. Constraints EQ1, EQ2, IN1, and IN3 were imposed on the optimization. A walking rate of 0.49 m/s (2 steps/sec) and a coefficient of friction of 0.65 were selected. For the optimization, m_m, m_9, the initial condition for $\dot{q}_m$, and the coefficients of the polynomial $h_d(\theta)$ (which describes the desired evolution of q_i) were chosen as the variable parameters. Upper and lower bounds were placed on the design variables such that (i) the link masses were physically realizable, (ii) the initial condition for $\dot{q}_m$ always resulted in forward motion, and (iii) the polynomial coefficients resulted in a strictly monotonic function of θ.

The parameters that resulted from optimization are: $|\vec{r}_b| = 0.080$ m, $|\vec{r}_i| = 0.021$ m, $|\vec{r}_3| = 0.108$ m, $|\vec{r}_4| = 0.074$ m, $|\vec{r}_5| = 0.056$ m, $|\vec{r}_6| = 0.192$ m, $|\vec{r}_7| = 0.128$ m, $|\vec{r}_m| = 0.248$ m, $|\vec{r}_9| = 0.248$ m, $m_b = 0.500$ kg, $m_i = 0.130$ kg, $m_3 = 0.068$ kg, $m_5 = 0.350$ kg, $m_6 = 0.120$ kg, $m_8 = 0.024$ kg, $m_m = 1.478$ kg, $m_9 = 0.468$ kg, and $\alpha_{mech} = 5.97$ rad. The acceleration due to gravity is $g_0 = 9.81$ m/s^2 and the total mass[4] of the robot is $M_{tot} = 6.275$ kg. Note

[4]The total mass of the robot does not include the mass of the motor and gearhead. Future work will include an analysis of the effects of these additional masses

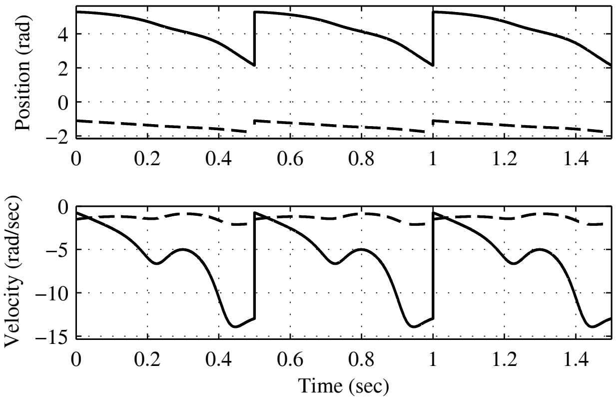

Fig. 4. Joint angles and velocities versus time. Trajectories of q_i (solid) and q_m (dashed) indicate that the motion is periodic. The walking rate is 0.49 m/s.

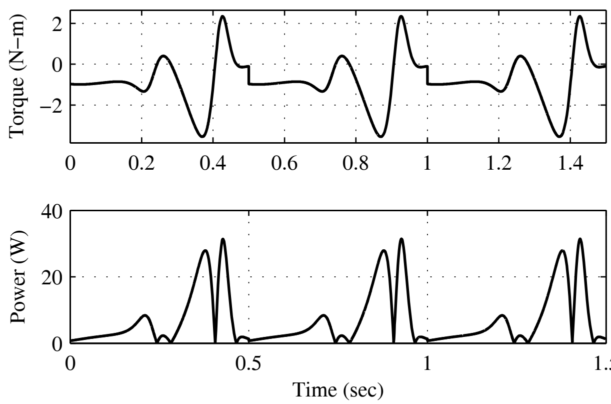

Fig. 5. Required actuator torque and absolute power versus time. The required peak actuator torque of 3.6 N-m and peak power requirement of 31.5 W are modest considering the mechanism's size and mass.

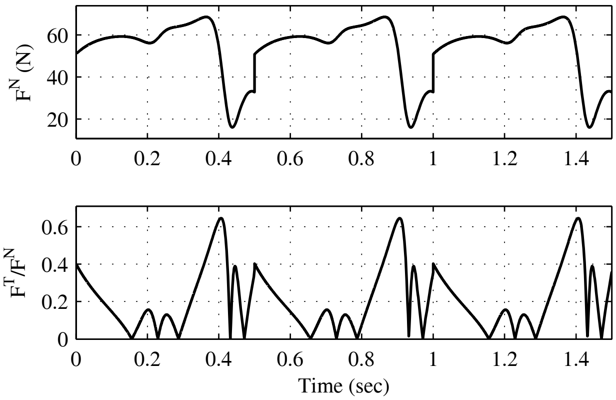

Fig. 6. Ground reaction forces versus time. The normal ground reaction force is always directed upward (positive), while the ratio of the tangential and normal components does not exceed a reasonable coefficient of friction (0.65).

that m_m corresponds to the total mass of $|\vec{r}_4|$ and $|\vec{r}_m|$ (a single, rigid link) and m_9 corresponds to the total mass of $|\vec{r}_7|$ and $|\vec{r}_9|$ (also a single, rigid link). Figures 4–6 are plots corresponding to a simulation of three steps of the mechanism with the parameters given. Plots of the joint angles and velocities are given in Figure 4, and the actuator torque and power required for this motion are presented in Figure 5. The ground reaction force plots are given in Figure 6.

A stability analysis was conducted as specified in Section III-G. Conditions (11) and (13) were met with $\zeta_2^{*-} = 0.76$ N-m-s and $\delta^2_{\text{zero}} = 0.60$.

V. Conclusions

This paper integrates kinematic mechanism design and hybrid system analysis to produce an algorithm for the design of a mechanically-coordinated, single-DOF biped robot that can achieve dynamic walking gaits that are stable. Requirements for the biped's design and dynamic analysis are presented along with methods for optimization. The example biped designed using this approach exhibits a stable walking gait and requires reasonable torques for the single actuator. The design is physically realizable and less complex than one whose DOF are coordinated by direct actuation. The methods presented in this paper are general and may be used for the design of other single-DOF bipeds that are able to achieve stable, dynamic walking gaits.

VI. Acknowledgements

This work was generously supported by National Science Foundation grant CMS-0408348.

References

[1] C. Chevallereau, G. Abba, Y. Aoustin, F. Plestan, E. R. Westervelt, C. Canudas, and J. W. Grizzle, "RABBIT: a testbed for advanced control theory," *IEEE Control Systems Magazine*, vol. 23, no. 5, pp. 57–79, Oct. 2003.

[2] S. H. Collins, A. Ruina, R. Tedrake, and M. Wisse, "Efficient bipedal robots based on passive-dynamic walkers," *Science*, vol. 307, pp. 1082–85, 2005.

[3] A. Goswami, "Postural stability of biped robots and the foot-rotation indicator (FRI) point," *International Journal of Robotics Research*, vol. 18, no. 6, pp. 523–33, June 1999.

[4] G. Kinzel and K. Waldron, *Kinematics, Dynamics, and Design of Machinery*, 2nd ed. Wiley, 1999.

[5] T. McGeer, "Passive dynamic walking," *International Journal of Robotics Research*, vol. 9, no. 2, pp. 62–82, Apr. 1990.

[6] K. Ono, T. Furuichi, and R. Takahashi, "Self-excited walking of a biped mechanism with feet," *International Journal of Robotics Research*, vol. 23, no. 1, pp. 55–68, 2004.

[7] L. Rygg, "Mechanical horse," *US Patent*, February 14 1893.

[8] J. P. Schmiedeler, E. R. Westervelt, and A. R. Dunki-Jacobs, "Integrated design and control of a biped robot," in *Proceedings of the 2005 ASME International Design Engineering Technical Conference*, Long Beach, CA, 2005.

[9] X. Wan and S.-M. Song, "A cam-controlled, single-actuator-driven leg mechanism for legged vehicles," in *Proceedings of the ASME International Mechanical Engineering Congress and Exposition*, Anaheim, California, 2004.

[10] E. R. Westervelt, J. W. Grizzle, C. Chevallereau, J.-H. Choi, and B. Morris, *Feedback Control of Dynamic Bipedal Robot Locomotion*. Taylor & Francis/CRC Press, 2007.

[11] E. R. Westervelt, J. W. Grizzle, and D. E. Koditschek, "Hybrid zero dynamics of planar biped walkers," *IEEE Transactions on Automatic Control*, vol. 48, no. 1, pp. 42–56, Jan. 2003.